

Enhanced Photocatalytic H₂-production Activity of CdS Nanoflower using Single Atom Pt and Graphene Quantum Dot as dual Cocatalysts

Yi Yang¹, Jinsong Wu¹, Bei Cheng^{1*}, Liuyang Zhang^{2*}, Ahmed Abdullah Al-Ghamdi³, Swelm Wageh³ and Youji Li⁴

¹State Key Laboratory of Advanced Technology for Materials Synthesis and Processing, Nanostructure Research Centre (NRC), Wuhan University of Technology, Wuhan 430070, China

²Laboratory of Solar Fuel, Faculty of Materials Science and Chemistry, China University of Geosciences, Wuhan 430074, China

³Department of Physics, Faculty of Science, King Abdulaziz University, Jeddah 21589, Saudi Arabia

⁴College of Chemistry and Chemical engineering, Jishou University, Jishou, Hunan 416000, China

*Corresponding authors. E-mails: chengbei2013@whut.edu.cn (Bei Cheng) and zhangliuyang@cug.edu.cn (Liuyang Zhang)

n EXPERIMENTAL

Material Characterization. X-ray diffraction (XRD) patterns were acquired on the Rigaku diffractometer (Japan) equipped with Cu K α radiation. The morphology was studied by a field-emission scanning electron microscopy (FESEM; JSM 7500F, JEOL, Japan) and a transmission electron microscopy TEM (Titan G2 60-300, FEI) with EDS equipment. The aberration-corrected HAADF-STEM characterization was conducted on a transmission electron microscope (Titan Cubed Themis G2 300). The thickness of the samples was obtained on an atomic force microscope (AFM; Multimode 8, Bruker, USA). The ultraviolet-visible diffuse reflectance absorption spectrum was investigated on a UV-vis spectrophotometer (UV-2600, Shimadzu, Japan). The Brunauer-Emmett-Teller (BET) specific surface area (S_{BET}) and pore size distribution of the powders were obtained by nitrogen adsorption in a nitrogen adsorption apparatus (TriStar II 3020, Micromeritics, USA). X-ray photoelectron spectroscopy (XPS) analysis was performed on a Thermo Scientific ESCALA 210 XPS spectrometer system (USA) with 300 W Al K α radiation to investigate the chemical composition of the samples and the chemical states of the elements. The binding energies were calibrated by the C 1s peak at 284.8 eV from adventitious carbon. Photoluminescence (PL) spectra of the samples were analyzed by a fluorescence spectrophotometer (F-7000, Hitachi, Japan) with the excitation wavelength at 420 nm. XANES and EXAFS spectra of Pt L_3 -edge were recorded at BL01C1 of the National Synchrotron Radiation Reaction Center (NSRRC).

Photoelectrochemical Measurements. Electrochemical measurements were measured on an electrochemical workstation (CHI660C, China) in a standard three-electrode system. The photoelectrodes were prepared as follows. 20 mg of powdered samples was dispersed into 20 μ L of Nafion and 300 μ L of ethanol under ultrasonication for 30 min. The as-prepared samples coated on an FTO glass acted as the working electrode with an active area of ca. 1.0 cm², whereas a Pt wire and Ag/AgCl (saturated KCl) were used as the counter and reference electrodes, respectively. 50 mL of 0.5 M Na₂SO₄ aqueous solution was selected as the electrolyte. A LED light (3 W, 420 nm) (Shenzhen LAMPLIC Science Co. Ltd. China) was used as the visible-light source. 50 mL of 0.5 M Na₂SO₄ aqueous solution was selected as the electrolyte.

Photocatalytic Performance Test. The photocatalytic H₂ production experiments were carried out in a 100 mL three-necked flask using a 350 W Xenon arc lamp as a visible-light source. The lamp with a UV cut-off filter (\geq 420 nm) was used to trigger the photocatalytic reaction. In a typical photocatalytic reaction, 20 mg photocatalyst was suspended in 80 mL of 10 vol% lactic acid aqueous solution. Before irradiation, the system was bubbled with nitrogen through the flask for 30 min to completely remove the dissolved oxygen. During the photocatalytic experiments, a 0.4 mL gas was sampled from the headspace of the reactor and the photocatalytic hydrogen evolution activity was analyzed by gas chromatography (GC-14C, Shimadzu, Japan) with a thermal conductivity detector. Besides, the stability experiment was conducted by repeating the above steps four times. The cycle was repeated every three hours, and N₂ was saturated for half an hour before the next cycle was started.

The apparent quantum efficiency (AQE) measurement was measured under the irradiation of four 420 nm LED lights with an irradiation density of 9.0 mW cm⁻². The AQE of photocatalytic H₂ production was calculated according to the following equation (1):

$$AQE = \frac{2 \times \text{number of evolved H}_2 \text{ molecules in unit time}}{\text{number of incident photons in unit time}} \times 100\% \quad (1)$$

The energy conversion efficiency (η_c) under a 350 W Xenon arc lamp with a UV cut-off filter (\geq 420 nm) was determined by equation (2), where ΔG^0 (J mol⁻¹) is the standard Gibbs energy for the hydrogen evolution reaction, R (mol s⁻¹) is the rate of hydrogen generation in its standard state, E_s (W cm⁻²) is the incident solar irradiance and A (cm²) is the irradiated area.^[1]

$$\eta_c = \Delta G^0 R / E_s A \quad (2)$$

Average Decay Time (τ_{average}). The average decay time (τ_{average}) was calculated from equation 3:

$$\tau_{\text{Average}} = \frac{A_1 \tau_1^2 + A_2 \tau_2^2}{A_1 \tau_1 + A_2 \tau_2} \quad (3)$$

Work Function. The work function (denoted as W) of the samples is calculated according to the following equation:

$$W_{\text{sample}} = e \times CPD_{\text{sample}} + W_{\text{probe}} \quad (4)$$

where W_{probe} is the work function (4.25 eV) of gold mesh probe, CPD_{sample} is the contact potential difference value of the sample, e is the electron charge, and W_{sample} is the work function of the tested sample.

Furthermore, the Fermi levels (E_f) of the samples are calculated as follows:

$$W_{\text{sample}} + E_f = E_{\text{vac}} \quad (5)$$

where W_{sample} is a work function, and E_{vac} is the energy of the vacuum level (0 eV).

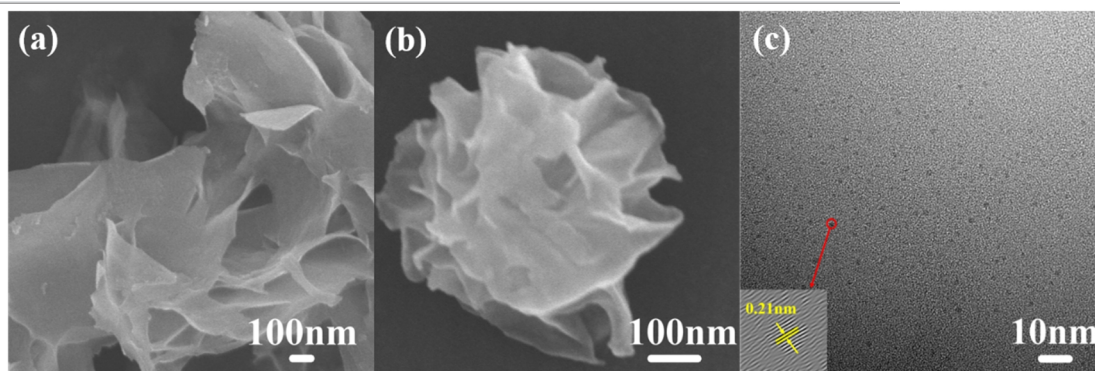


Figure S1. (a) Magnified FESEM image of the CdS nanosheets; (b) FESEM image of CdS/GQDs/PtSAs; (c) TEM image of GQDs.

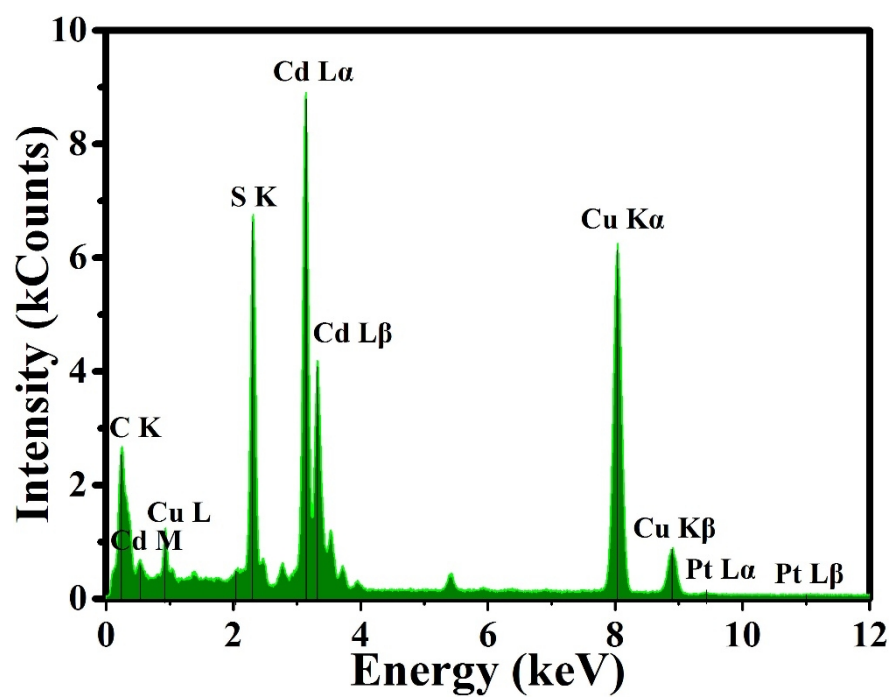


Figure S2. EDS spectrum of CdS/GQDs/PtSAs.

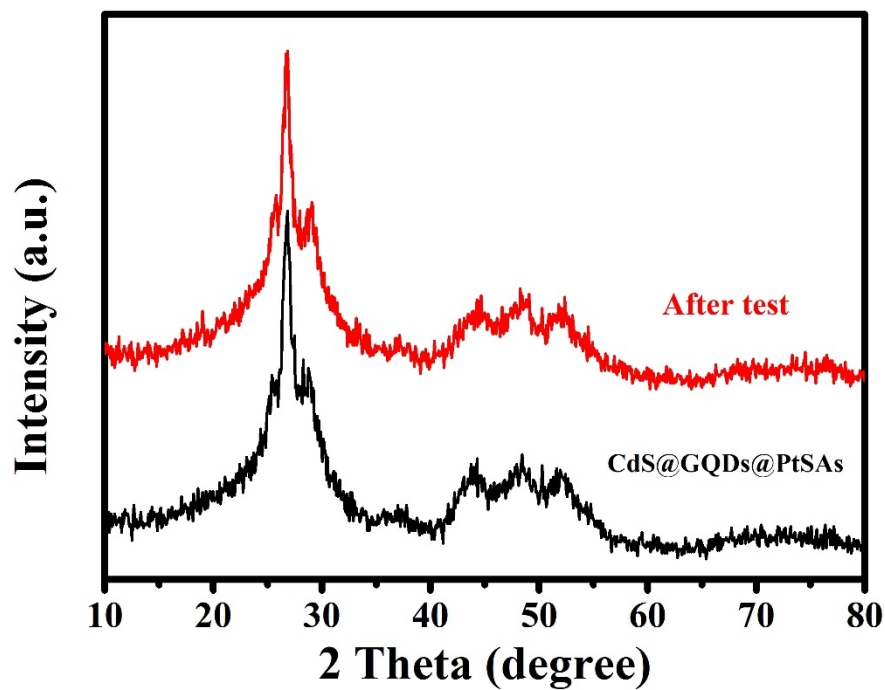


Figure S3. XRD patterns of CdS/GQDs/PtSAs before and after cyclic photocatalytic reactions.

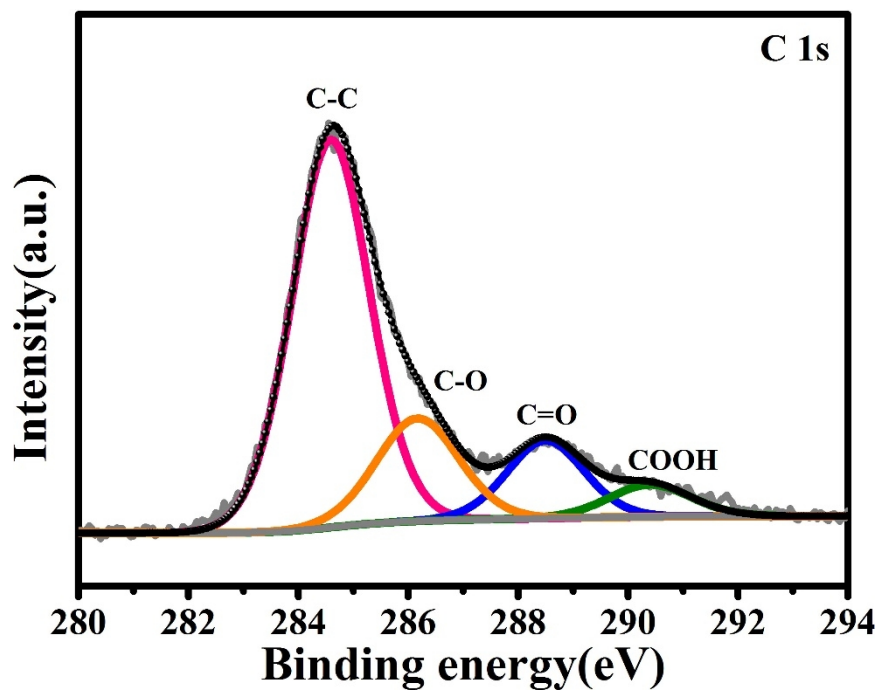


Figure S4. High-resolution X-ray photoelectron spectra of C 1s regions.

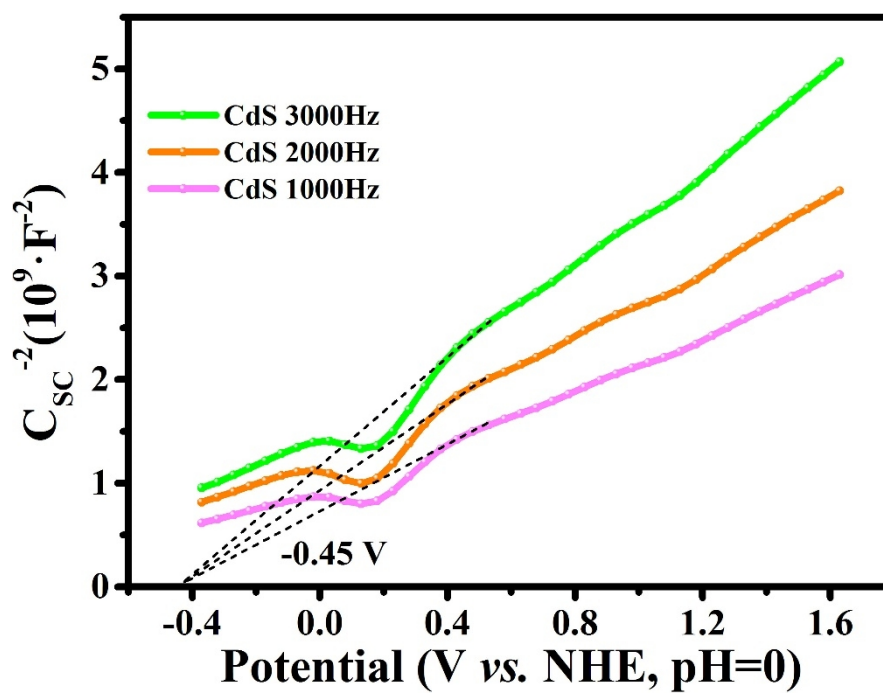


Figure S5. Mott-Schottky curves of CdS.

Table S1. Performance Comparison of CdS-based Photocatalysts for H₂ Production

| Photocatalysts | Light source | Yield | Reference |
|--|--|---|-----------|
| CdS/GQDs/PtSAs | 350W Xe lamp, $\lambda > 420$ nm | 13.48 mmol g ⁻¹ h ⁻¹ | This work |
| MoS ₂ /Graphene-CdS | 300W Xe lamp, $\lambda > 420$ nm | 1.6 mmol h ⁻¹ | [2] |
| CdS-700Ni@ Graphene | 300W Xe lamp, $\lambda > 420$ nm | 5.9 mmol g ⁻¹ h ⁻¹ | [3] |
| CdS@MoS ₂ | Vis-light illumination ($\lambda > 400$ nm) | 404 μ mol h ⁻¹ | [4] |
| CdS/Ni ₂ P | Vis-light illumination | 33480 μ mol h ⁻¹ g ⁻¹ | [5] |
| MoC/CdS | 300W Xe lamp, $\lambda > 420$ nm | 224.5 μ mol h ⁻¹ | [6] |
| rGO-CdS@MoS ₂ | Visible light ($420 < \lambda < 780$ nm) | 14.4 mmol g ⁻¹ h ⁻¹ | [7] |
| Pt/CdS | Vis-light illumination ($\lambda > 400$ nm) | 13.0 mmol g ⁻¹ h ⁻¹ | [8] |
| Pt/Mo ₂ C/CdS | 300W Xe lamp, $\lambda > 420$ nm | 8090 μ mol g ⁻¹ h ⁻¹ | [9] |
| Mo ₂ N/Mo ₂ C/GR/CdS | 300W Xe lamp, $\lambda > 420$ nm | 4520 μ mol g ⁻¹ h ⁻¹ | [10] |
| CdS/WSx | 300W Xe lamp, $\lambda > 420$ nm | 760.8 μ mol h ⁻¹ | [11] |
| CdS/VC | 300W Xe lamp, $\lambda > 420$ nm | 14.2 mmol h ⁻¹ g ⁻¹ | [12] |
| 2%Ni ₂ P/CdS | 300W Xe lamp, $\lambda > 400$ nm | 0.91 mmol·h ⁻¹ | [13] |

n REFERENCES

- (1) J. Zhang, J. Yu, M. Jaroniec, J. R. Gong, Noble metal-free reduced graphene oxide-Zn_xCd_{1-x}S nanocomposite with enhanced solar photocatalytic H₂-production performance. *Nano Lett.* **2012**, 12, 4584-4589.
- (2) K. Chang, Z. Mei, T. Wang, Q. Kang, S. Ouyang, J. Ye, MoS₂/Graphene cocatalyst for efficient photocatalytic H₂ evolution under visible light irradiation. *ACS Nano* **2014**, 8, 7078-7087.
- (3) T. Di, L. Zhang, B. Cheng, J. Yu, J. Fan, CdS nanosheets decorated with Ni@graphene core-shell cocatalyst for superior photocatalytic H₂ production. *J. Mater. Sci. Technol.* **2020**, 56, 170-178.
- (4) X. Fu, L. Zhang, L. Liu, H. Li, S. Meng, X. Ye, S. Chen, In situ photodeposition of MoS_x on CdS nanorods as a highly efficient cocatalyst for photocatalytic hydrogen production. *J. Mater. Chem. A* **2017**, 5, 15287-15293.
- (5) D. P. Kumar, J. Choi, S. Hong, D. A. Reddy, S. Lee, T. K. Kim, Rational synthesis of metal-organic framework-derived noble metal-free nickel phosphide nanoparticles as a highly efficient cocatalyst for photocatalytic hydrogen evolution. *ACS Sustain. Chem. Eng.* **2016**, 4, 7158-7166.
- (6) Y. Lei, X. Wu, S. Li, J. Huang, K. H. Ng, Y. Lai, Noble-metal-free metallic MoC combined with CdS for enhanced visible-light-driven photocatalytic hydrogen evolution. *J. Cleaner Prod.* **2021**, 322, 129018.
- (7) Q. Liu, S. Wang, Q. Ren, T. Li, G. Tu, S. Zhong, Y. Zhao, S. Bai, Stacking design in photocatalysis: synergizing cocatalyst roles and anti-corrosion functions of metallic MoS₂ and graphene for remarkable hydrogen evolution over CdS. *J. Mater. Chem. A* **2021**, 9, 1552-1562.
- (8) X. Lu, A. Tong, D. Luo, F. Jiang, J. Wei, Y. Huang, Z. Jiang, Z. Lu, Y. Ni, Confining single Pt atoms from Pt clusters on multi-armed CdS for enhanced photocatalytic hydrogen evolution. *J. Mater. Chem. A* **2022**, 10, 4594-4600.
- (9) L. Luo, D. Li, Y. Dang, W. Wang, G. Yu, J. Li, B. Ma, Capacitance catalysis: positive and negative effects of capacitance of Mo₂C in photocatalytic H₂ evolution. *ACS Sustain. Chem. Eng.* **2022**, 10, 5949-5957.
- (10) B. Ma, X. Wang, K. Lin, J. Li, Y. Liu, H. Zhan, W. Liu, A novel ultraefficient non-noble metal composite cocatalyst Mo₂N/Mo₂C/graphene for enhanced photocatalytic H₂ evolution. *Int. J. Hydrogen Energy* **2017**, 42, 18977-18984.
- (11) S. Min, Y. Lei, H. Sun, J. Hou, F. Wang, E. Cui, S. She, Z. Jin, J. Xu, X. Ma, Amorphous WS_x as an efficient cocatalyst grown on CdS nanoparticles via photochemical deposition for enhanced visible-light-driven hydrogen evolution. *Mol. Catal.* **2017**, 440, 190-198.
- (12) L. Tian, S. Min, F. Wang, Integrating noble-metal-free metallic vanadium carbide cocatalyst with CdS for efficient visible-light-driven photocatalytic H₂ evolution. *Appl. Catal. B-Environ.* **2019**, 259, 118029.
- (13) Z. Wang, Z. Qi, X. Fan, D. Y. C. Leung, J. Long, Z. Zhang, T. Miao, S. Meng, S. Chen, X. Fu, Intimately contacted Ni₂P on CdS nanorods for highly efficient photocatalytic H₂ evolution: new phosphidation route and the interfacial separation mechanism of charge carriers. *Appl. Catal. B-Environ.* **2021**, 281, 119443.